Pramana – J. Phys. (2016) 87: 29
DOI 10.1007/s12043-016-1226-6

Quantum ring states in magnetic field and delayed half-cycle pulses

KRITI BATRA[1,*], HIRA JOSHI[2] and VINOD PRASAD[3]

[1]University School of Basic and Applied Sciences, G.G.S. Indraprastha University, Delhi 110 078, India
[2]Department of Physics, Gargi College, University of Delhi, Delhi 110 049, India
[3]Department of Physics, Swami Shraddhanand College, University of Delhi, Delhi 110 036, India
*Corresponding author. E-mail: kriti.ipu@gmail.com

MS received 10 October 2014; revised 1 November 2015; accepted 18 November 2015; published online 19 July 2016

Abstract. The present work is dedicated to the time evolution of excitation of a quantum ring in external electric and magnetic fields. Such a ring of mesoscopic dimensions in an external magnetic field is known to exhibit a wide variety of interesting physical phenomena. We have studied the dynamics of the single electron quantum ring in the presence of a static magnetic field and a combination of delayed half-cycle pulse pair. Detailed calculations have been worked out and the impact on dynamics by variation in the ring radius, intensity of external electric field, delay between the two pulses, and variation in magnetic field have been reported. A total of 19 states have been taken and the population transfer in the single electron quantum ring is studied by solving the time-dependent Schrödinger equation (TDSE), using the efficient fourth-order Runge–Kutta method. Many interesting features have been observed in the transition probabilities with the variation of magnetic field, delay between pulses and ring dimensions. A very important aspect of the present work is the persistent current generation in a quantum ring in the presence of external magnetic flux and its periodic variation with the magnetic flux, ring dimensions and pulse delay.

Keywords. Quantum ring; persistent current; magnetic flux; Aharonov–Bohm effect.

PACS Nos 73.21.−b; 73.23.Ra; 73.22.Dj

1. Introduction

For the past three decades, low-dimensional electron systems such as quantum dots and rings have been the subject of considerable interest and studied extensively. Due to their small size, these systems are governed by quantum effects and their energy spectra are discrete. They are in many ways similar to atoms. However, their properties can be controlled by adjusting their geometries, the confinement and the applied magnetic field. These nanostructures are a source of discoveries of intriguing quantum phenomena which do not appear in atoms [1–23]. They are important in connection with the potential device applications. They can also function as convenient samples to probe the properties of many electron systems in reduced dimensions. The quantum ring is a system of electrons confined to a circular region. Such a ring of mesoscopic dimensions in an external magnetic field is known to exhibit a wide variety of interesting physical phenomena. Electrons confined to a submicron ring manifest a quantum interference phenomenon known as the Aharonov–Bohm [24–26] effect originating because of the periodic dependence of the electronic phase on the magnetic flux through the ring. As a result, there is oscillatory behaviour in the energy levels which is a function of the applied magnetic field. This behaviour is usually associated with the occurrence of oscillatory currents in the ring [27,28]. The possibility of persistent current was predicted in the very early days of quantum mechanics by Hund [29], but the experimental evidences came much later, only after the realization of mesoscopic systems. Several experiments have confirmed the existence of persistent current [30,31]. Theoretical predictions have confirmed the periodicity in the persistent current in the presence of magnetic flux with a period of the flux quantum $\phi_0 = h/e$ [32–34]. Experimental evidence for Aharonov–Bohm oscillations has been seen in the mesoscopic regime in metallic rings [35–37]. Beltran *et al* have measured persistent current in normal metal rings under different magnetic fields and worked out magnetization [35]. Wenzler *et al* considered the Aharonov–Bohm effect in metal rings in the presence of CW RF excitation to modify decoherence time [38]. Similar results for semiconducting rings [39,40] have also been reported.

In the present work, we have considered a single electron one-dimensional (1D) quantum ring of radius r_0 placed in an external magnetic field and subjected to a combination of delayed half-cycle pulses. A 1D quantum ring in its ground state exhibits a circulating current (persistent current) when placed in an external magnetic field perpendicular to the plane of the ring. In addition, we have also subjected the ring to an external electromagnetic perturbation, and have found that the persistent current can be changed non-adiabatically as the single-electron state changes.

2. Theory and computation

We consider a one-dimensional quantum ring of radius r_0 carrying a single electron placed in an external magnetic field perpendicular to the plane of the ring. The ring is described by the following Hamiltonian operator:

$$H_0 = \frac{1}{m^*}(\mathbf{p} + e\mathbf{A})^2, \tag{1}$$

where m^* is the effective mass of the electron, $\mathbf{p}$ is the momentum of the electron and $\mathbf{A}$ is the vector potential describing the magnetic field $\mathbf{B}$

$$\mathbf{B} = \nabla \times \mathbf{A}. \tag{2}$$

Assuming that the magnetic field is constant and perpendicular to the plane of the ring, the vector potential can be expressed in the symmetric gauge

$$\mathbf{A} = -\frac{1}{2}\mathbf{r} \times \mathbf{B} = \frac{r_0 B}{2}\hat{e}_\theta, \tag{3}$$

where $\hat{e}_\theta$ is a unit vector in the plane of the ring and B is the magnitude of the magnetic field, $B = |\mathbf{B}|$. In polar coordinates, the Hamiltonian becomes

$$H_0 = -\frac{\hbar^2}{2m^* r_0^2}\left[\frac{\partial^2}{\partial\theta^2} + \iota\frac{eBr_0^2}{\hbar}\frac{\partial}{\partial\theta} - \left(\frac{eBr_0^2}{2\hbar}\right)^2\right]. \tag{4}$$

The polar angle θ specifies the angular position of the charge carrier with respect to the x-axis. Using the magnetic flux

$$\phi = \mathbf{B} \cdot \mathbf{S} = B\pi r_0^2, \tag{5}$$

as well as the flux quantum $\phi_0 = h/e$, the Hamiltoninan can be simplified to the form

$$H_0 = -\frac{\hbar^2}{2m^* r_0^2}\left[\frac{\partial^2}{\partial\theta^2} + \iota\frac{\phi}{\phi_0}\frac{\partial}{\partial\theta} - \left(\frac{\phi}{\phi_0}\right)^2\right]. \tag{6}$$

The time-independent Schrödinger equation of the system

$$\hat{h}_0|\Phi\rangle = \epsilon|\Phi\rangle, \tag{7}$$

has a known analytical solution and on imposing the boundary condition $\Phi(\theta + 2\pi) = \Phi(\theta)$, one finds that the eigenvalues of the Hamiltonian are restricted to a discrete set of allowed values. The wave functions and single-particle energy spectrum of the one-dimensional ring in the mth state are thus found to be

$$\langle\mathbf{r}|m\rangle = \Phi_m(\theta) = \frac{e^{-\iota m\theta}}{\sqrt{2\pi r_0}} \tag{8}$$

and

$$\epsilon_m = \frac{\hbar^2}{2m^* {r_0}^2}(m + m_\phi)^2, \tag{9}$$

where $m_\phi = \phi/\phi_0$ is the number of flux quanta piercing the ring.

The unperturbed Hamiltonian H_0 described above is symmetric under any rotational transformation. Consequently, H_0 commutes with the angular momentum operator L_z. The wave functions are the eigenfuctions of the z component of the angular momentum L_z, whose eigenvalues are determined by the quantum number m

$$L_z|m\rangle = -m\hbar|m\rangle. \tag{10}$$

Therefore, m also represents the z component of the angular momentum of the state. The set of wave functions forms a complete orthonormal basis

$$\langle l|m\rangle = \delta_{lm},\ \Sigma_m|m\rangle\langle m| = 1. \tag{11}$$

The energy spectrum defined by eq. (9) is shown in figure 1. It exhibits oscillations in the magnetic flux. One can see intersections (degeneracy) in the energy levels with different angular momenta when ϕ is equal to an integer number of $\phi_0/2$. For typical nanoscale rings [41,42] the energy scale of the interlevel separation lies in the THz range.

An important aspect of the study is the modifications in the electron dynamics in the presence of an external perturbation which in our case is a pulse pair consisting of a half-cycle pulse (HCP) and a second delayed pulse. At time $t = 0$, when the external perturbation

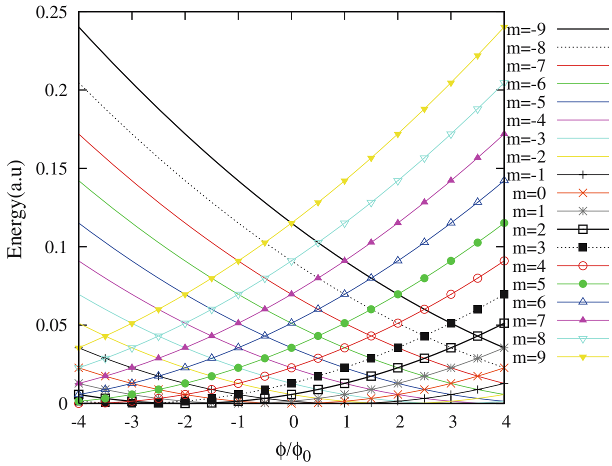

Figure 1. Energy levels of a single-electron one-dimensional quantum ring of radius $r_0 = 200$ Å as a function of m_ϕ.

is turned on, the Hamiltonian of the system becomes time-dependent

$$H(t) = H_0 + H_R(t,\theta), \tag{12}$$

with $H_R(t,\theta)$ defined by

$$H_R(t,\theta) = W(t)V(\theta), \tag{13}$$

$$W(t) = E_0 f(t)\cos(\omega t), \tag{14}$$

where E_0 is the amplitude of the electric field, ω is the frequency of the applied field of the HCP with duration t_{pi}, $f(t)$ is the envelop of the pulse defined by

$$f(t) = \sum_{i=1}^{2} \sin^2(\pi(t - t_{ci})/t_{pi}); \quad t_{ci} < t < t_{ci} + t_{pi} \tag{15}$$

$$f(t) = 0; \quad \text{otherwise.} \tag{16}$$

We have applied a combination of delayed half-cycle pulses with pulse duration t_{pi} and a delay of t_{ci} bet ween the two pulses. For the first pulse $t_{c1} = 0$. The pulse duration has been taken to be 0.1 ps which is small with respect to its rotational time period, hence non-adiabatic interaction is observed. The spatial component of the external pulse $V(\theta)$ is given by a combination of a dipole and a rotated quadrupole with amplitude A:

$$V(\theta) = A(\cos\theta + \cos 2\theta). \tag{17}$$

An eigenfunction of the time-dependent Hamiltonian (12) which maintains the 2π periodicity in θ can be written as a linear combination of the wave function (8)

$$\Psi_n(\theta) = N \sum_m c_m^n \mathrm{e}^{\iota m\theta}, \tag{18}$$

where N is the normalization constant.

The time-dependent Schrödinger equation

$$\iota \frac{\partial \Psi_n(\theta,t)}{\partial t} = H(t,\theta)\Psi_n(\theta,t) \tag{19}$$

is obtained by substituting the wave function (19) into the Schrödinger equation with Hamiltonian (12). A total of 19 states have been taken and the results have been converged with respect to the number of states. The above equation is solved numerically using fourth-order Runge–Kutta method with initial condition taken as the system being in the ground state for $m(0) = 1$, where states are from $m = -9$ to $+9$.

Another important aspect of the study is the generation of persistent current in the quantum ring in the presence of external magnetic flux. The current density within the ring is given by

$$j_0 = \frac{\iota\hbar}{2m^*}[(\Psi \bigtriangledown \Psi^*) - (\Psi^* \bigtriangledown \Psi)]. \tag{20}$$

Substituting eq. (18) into (20)

$$j_0 = \frac{\iota\hbar}{2m^*} \sum_n \sum_m \frac{\iota(n-m)C_n C_m^* \mathrm{e}^{\iota(n-m)\theta}}{r_0}. \tag{21}$$

The variation in the persistent current density has been studied as a function of all the input parameters, viz.

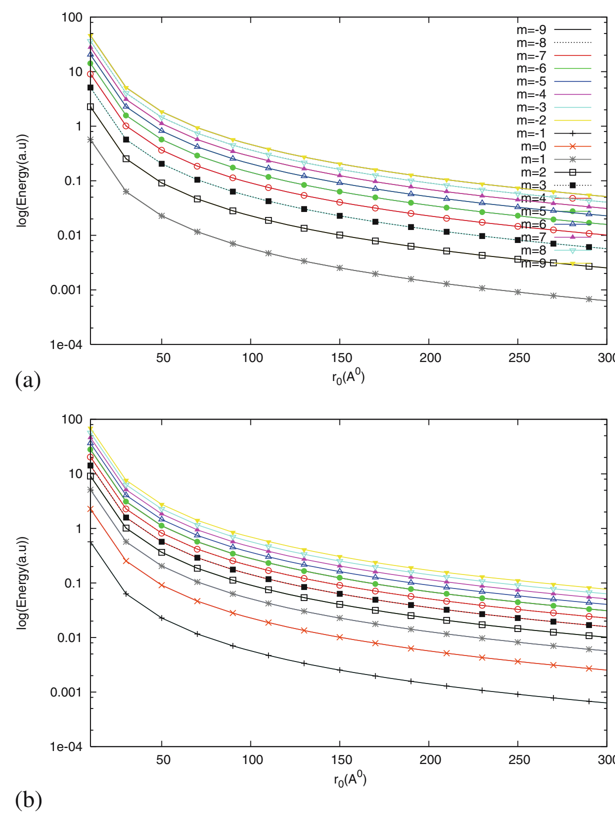

Figure 2. Energy levels of a single-electron one-dimensional quantum ring as a function of ring radius for (**a**) $m_\phi = 0$ and (**b**) $m_\phi = 2$ plotted on log scale.

ring dimensions, magnetic field and the delay between the pulses, and interesting results have been obtained.

3. Results and discussion

We have studied the impact of a combination of static magnetic field and a combination of delayed half-cycle pulses on a single electron semiconductor quantum ring. We have calculated all the results by taking gallium arsenide as the test material and have taken the effective mass as 0.067 times the free electron mass. In this study, we have taken a total of 19 states from $m = -9$ to $m = +9$ and the results have been converged with respect to the number of these states.

Figure 1 is a plot of the energies of a single electron quantum ring by varying the magnetic flux for a constant ring radius ($r_0 = 200$ Å). As can be seen from the graph, the states $m = -9, 9$, $m = -8, 8, \ldots, m = -1, 1$ are degenerate at $\phi/\phi_0 = 0$ but in the presence of external magnetic field this degeneracy is shifted in units of flux quanta. The energy levels are periodic in the number of flux quanta threading the ring and are even functions of ϕ/ϕ_0 for the ground state $m = 0$. It can be seen from the graph that in the ground state the energy of the quantum ring increases with increase in the magnetic field. For all other excited states, the energy of a $+m$th state at $+m_\phi$ is the same as the energy of the $-m$th state at $-m_\phi$. Similar behaviour of the energy spectrum can also be seen in the work of other researchers [43–45].

Figure 2 shows the dependence of the energy eigenvalues on the dimensions of the ring. Results are plotted for zero (figure 2a) as well as finite values of m_ϕ (figure 2b). As shown in the graph, the energy increases significantly for small r_0 but increases slowly for large values of r_0 which represents a quantum

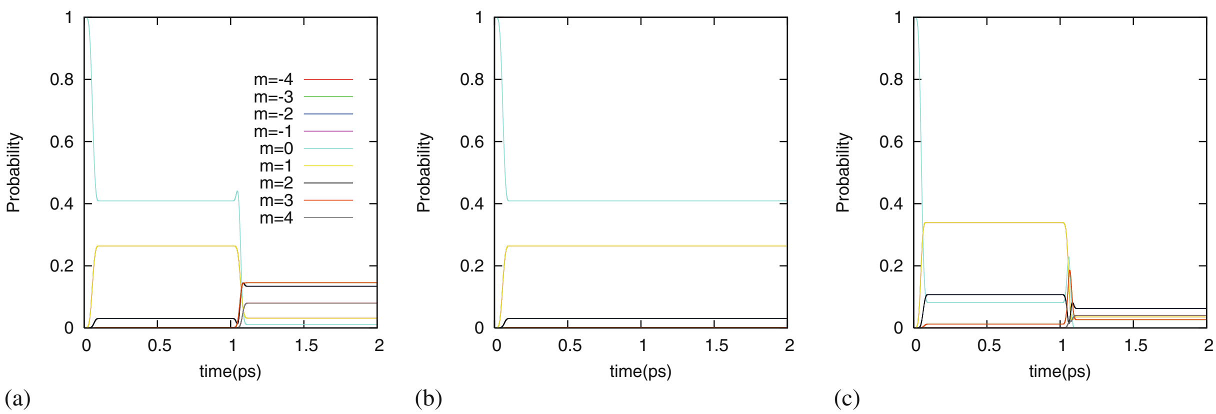

Figure 3. Transition probability as a function of time plotted for states from $m = -4$ to $m = +4$ for a single-electron quantum ring with $r_0 = 200$ Å and $m_\phi = 0$ with (**a**) electric field intensity $E_0 = 1.0 \times 10^6$ V/cm for both pulses with pulse duration $t_p = t_{pp} = 0.1$ ps and pulse delay $= 0.71 t_{\mathrm{rot}}$, (**b**) $E_0 = 1.0 \times 10^6$ V/cm single pulse case, (**c**) $E_0 = 1.5 \times 10^6$ V/cm for both pulses with $t_p = t_{pp} = 0.1$ ps and pulse delay $= 0.71 t_{\mathrm{rot}}$.

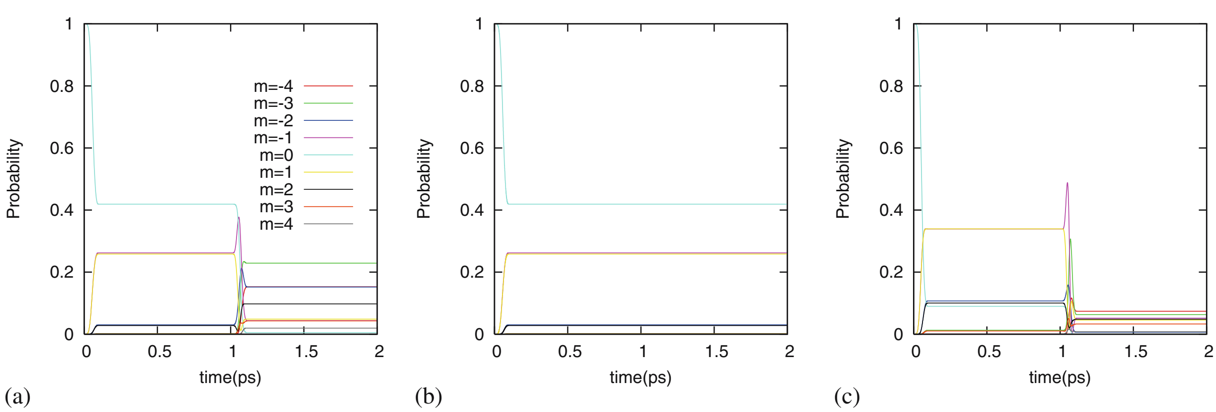

Figure 4. Transition probability as a function of time plotted for states from $m = -4$ to $m = +4$ for a single electron quantum ring with $r_0 = 200$ Å and $m_\phi = 2$ with (**a**) electric field intensity $E_0 = 1.0 \times 10^6$ V/cm for both pulses with pulse duration $t_p = t_{pp} = 0.1$ ps and pulse delay $= 0.71 t_{\mathrm{rot}}$, (**b**) $E_0 = 1.0 \times 10^6$ V/cm single pulse case, (**c**) $E_0 = 1.5 \times 10^6$ V/cm for both pulses with $t_p = t_{pp} = 0.1$ ps and pulse delay $= 0.71 t_{\mathrm{rot}}$.

confinement for smaller ring dimensions. This type of quantum confinement has earlier been reported by a couple of researchers [46,47].

An interesting aspect of the present work is the study of transition probabilities of the electron in various states under the influence of magnetic field. Figure 3 shows the variation of transition probabilities (in the absence of magnetic field) of the states from $m = -4$ to $m = +4$ (other states being insignificant) as a function of time. Figure 3a is a plot in the presence of delayed half-cycle pulse pair of the electric field $E_0 = 1.0 \times 10^6$ V/cm with a time delay between the two pulses of $t_c = 0.71 t_R$ with t_R being the rotational time period, figure 3b is for a single pulse with the same E_0 as in figure 3a and figure 3c is for delayed half-cycle pulse pair with higher peak amplitude $E_0 = 1.5 \times 10^6$ V/cm and the same t_c as in figure 3a. At time $t = 0$, $m = 0$ is taken as the

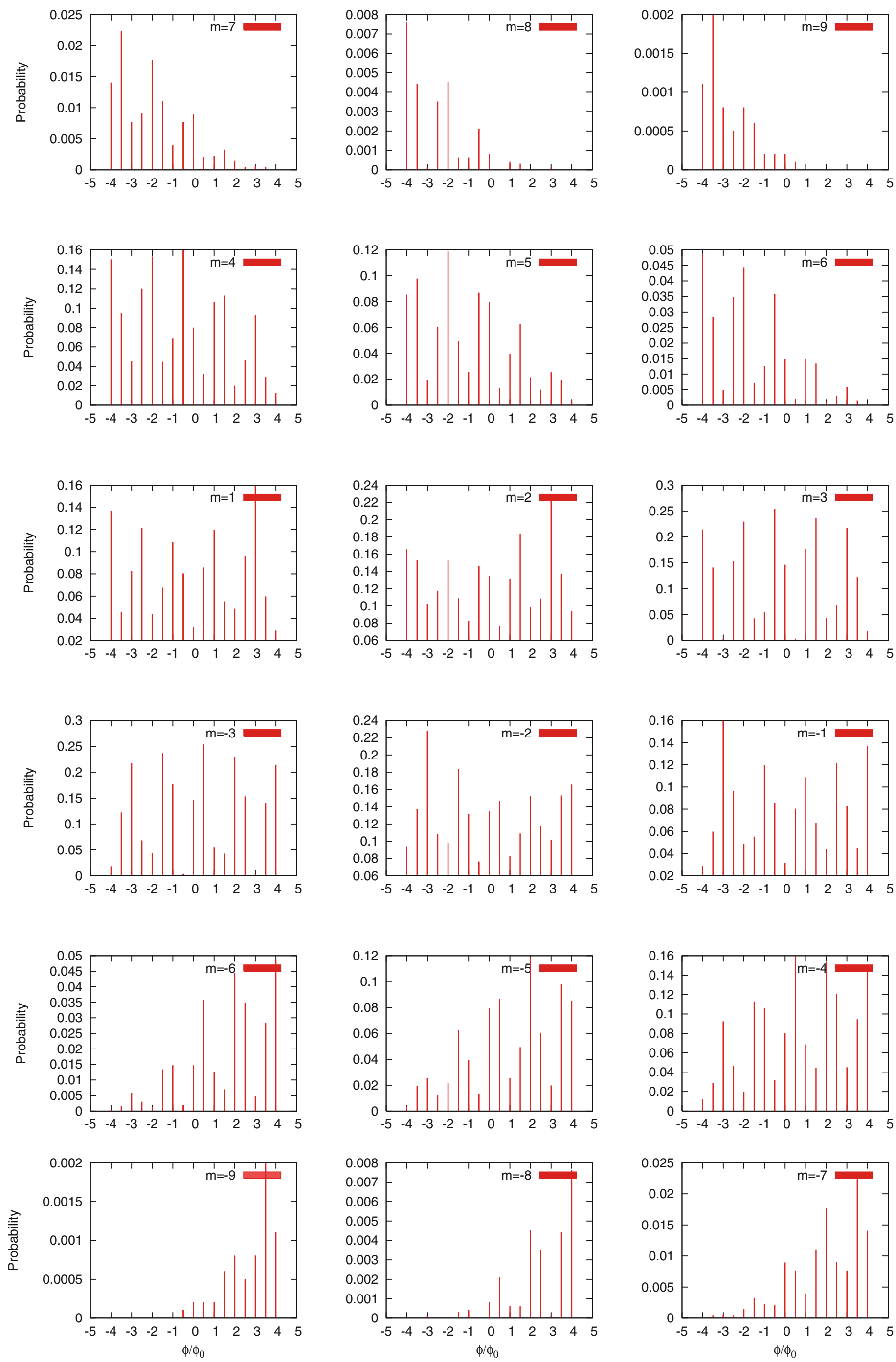

Figure 5. End of pulse transition probability for states $m = \pm 1$ to ± 9 vs. ϕ/ϕ_0 for a ring of radius = 200 Å.

ground state. The probability flows to other levels more prominently than to the adjacent levels. In the absence of external magnetic field, there is an equal probability for the $+m$ and $-m$ transitions. For a pure one-electron quantum ring, the dipole-allowed transition from the ground state can happen with equal probability to the first two excited states and all other transitions are forbidden which is apparent from figure 3b plotted for a single pulse case. The effect of the arrival of the second pulse is apparent by the modification in transition probabilities. Similar results are plotted in figure 4 for a finite value of $m_\phi = 2$. The degeneracy of the states is shifted by the applied static magnetic field which mixes the angular momentum eigenstates of the pure system into new states between which dipole transitions are allowed. The modification in dynamics with the arrival of the second pulse is shown in figures 4a and 4c.

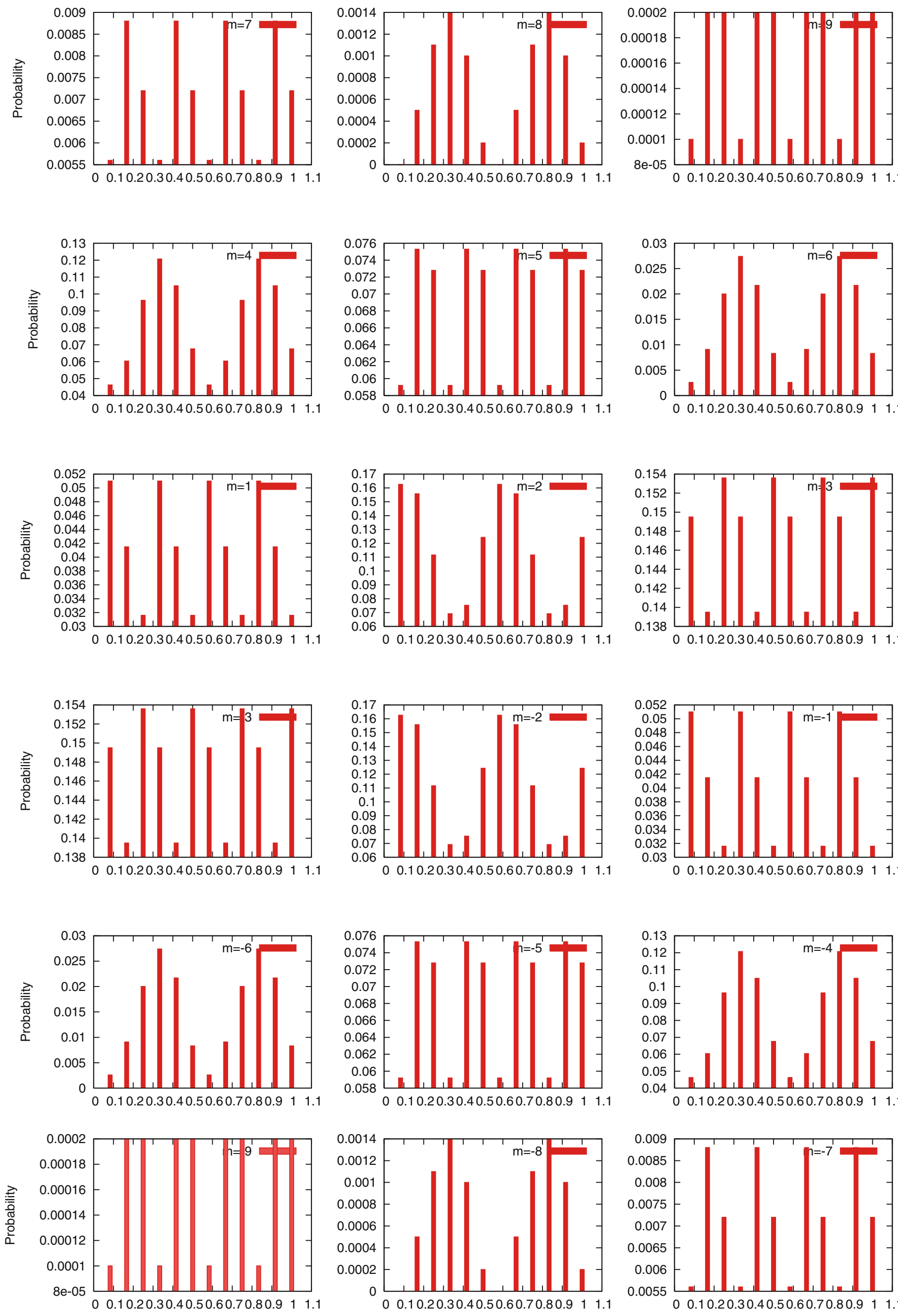

Figure 6. Variation of transition probability with pulse delay between two pulses of equal width = 0.1 ps when $E_0 = 1.0 \times 10^6$ V/cm and $m_\phi = 0$.

Figure 5 is a plot of the probabilities of all the 18 states at the end of the pulse as a function of the flux quanta ϕ/ϕ_0. It can be seen that as the magnetic flux is threading the ring, the $+m$ state is a mirror image of the $-m$ state. The probability for an mth state at a particular value of ϕ/ϕ_0 is the same as the $-m$th state at a value of $-\phi/\phi_0$ and the probabilities are oscillating with m_ϕ.

Figure 6 shows how transition probabilities get affected by a change in pulse delay. The end of the pulse probabilities for $m = \pm 9$ to $m = \pm 1$ states as function of the time delay between the two pulses is plotted. As can be seen, within the rotational period, the probabilities are oscillating with t_c in a periodic fashion. Also the flow to the $\pm m$th level is totally symmetric in the absence of the static magnetic field. In all these calculations, peak amplitude is taken as

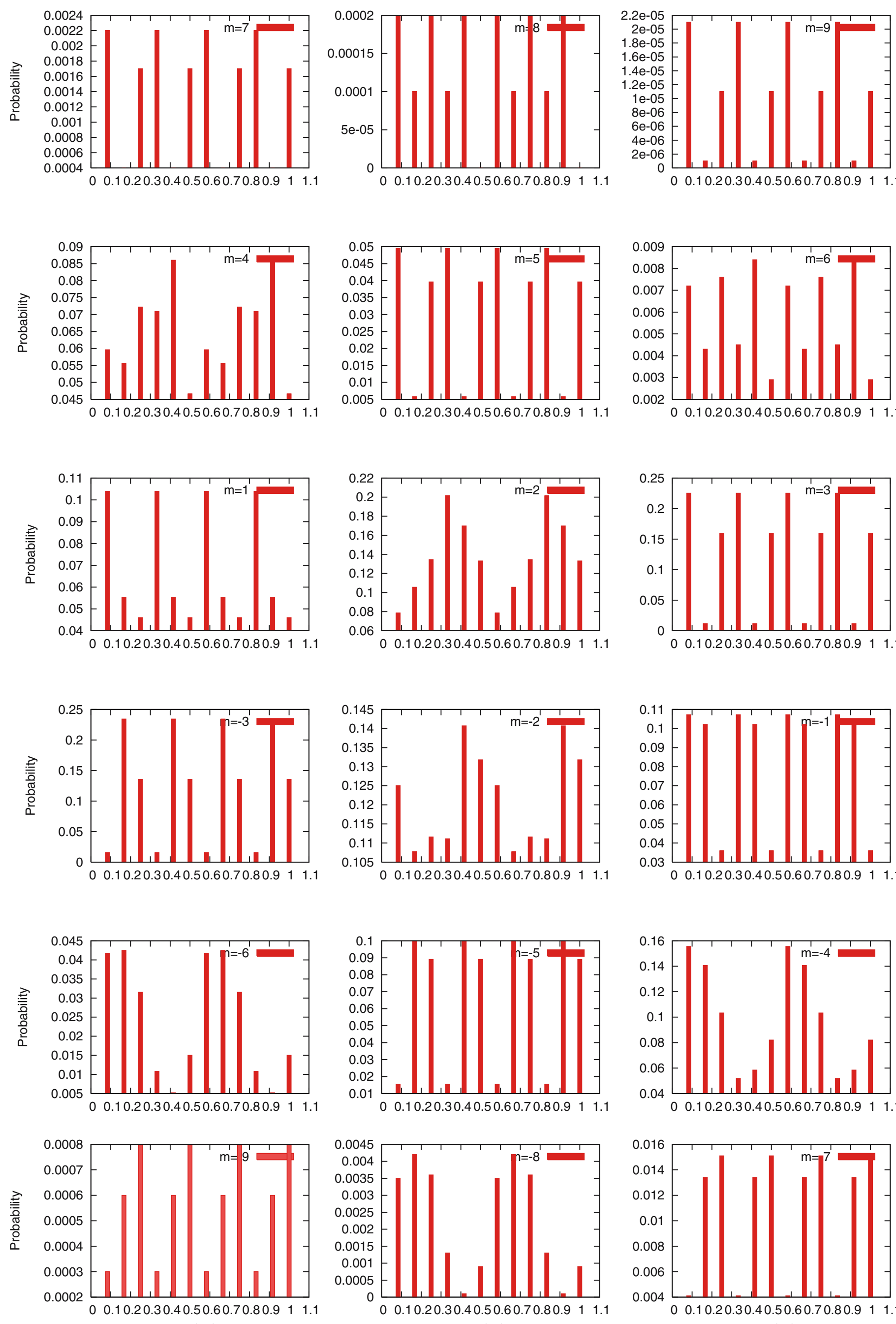

Figure 7. Variation of transition probability with pulse delay between two pulses of equal width $= 0.1$ ps when $E_0 = 1.0 \times 10^6$ V/cm and $m_\phi = 2$.

$E_0 = 1.0 \times 10^6$ V/cm and a constant ring radius of 200 Å is taken. Similar results in the presence of the static magnetic field m_ϕ are plotted in figure 7.

With the help of figure 8, a study has been made to optimize the ring radius for the excitation of a particular state. Figure 8 is a plot of the probabilities of all the excited states as a function of ring radius in the presence of the static magnetic field.

Further calculations have been done to work out the persistent current density in the ring. Figure 9 is a graphical representation of the current density in the quantum ring as a function of the external magnetic flux for two different ring dimensions and at two different intensities. It has been found to be periodic in magnetic flux threading the ring. In figure 10, current density has been plotted as a function of ring dimensions

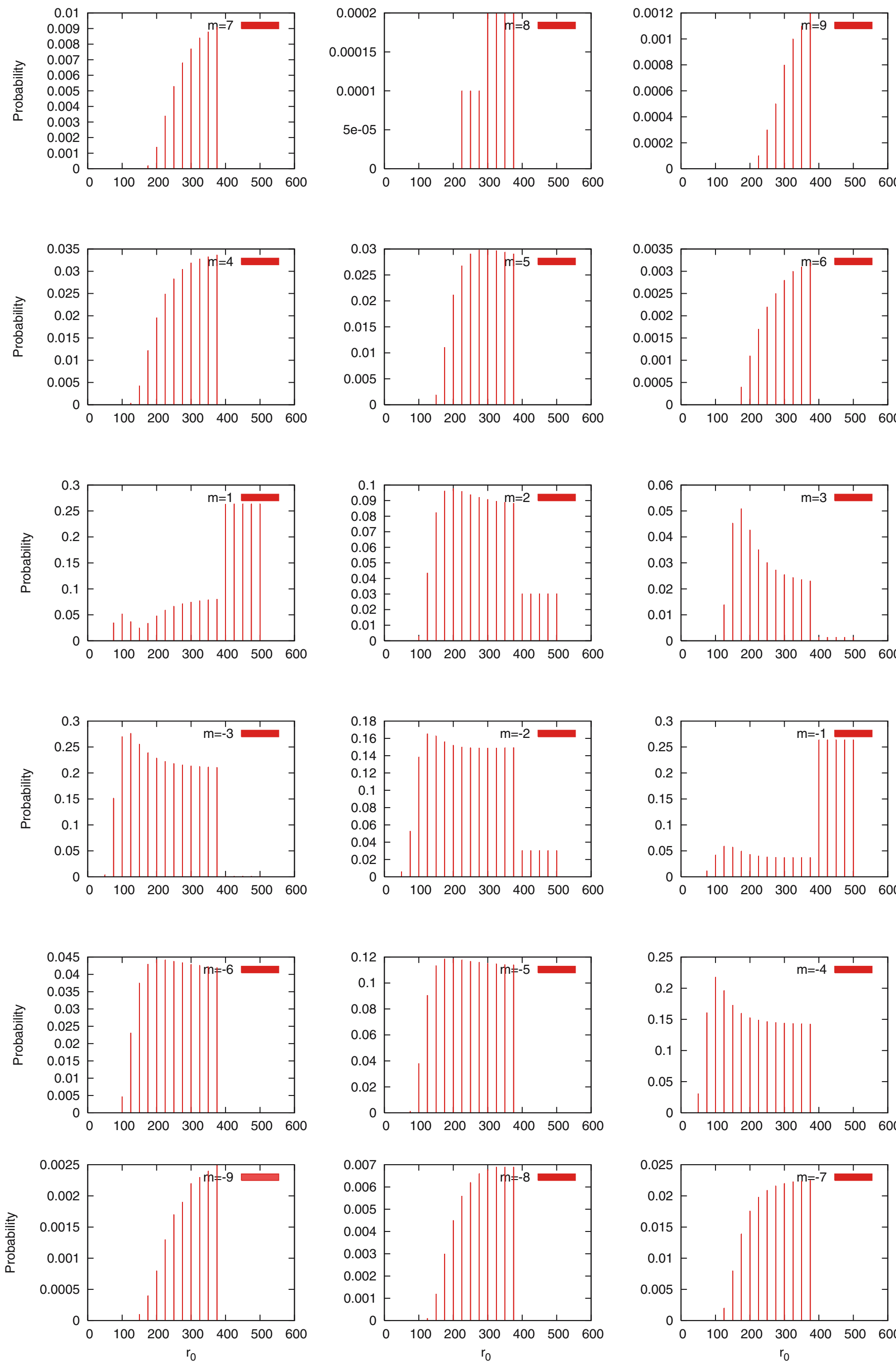

Figure 8. Variation of transition probability as a function of ring dimensions in the presence of delayed pulses of equal width = 0.1 ps when $E_0 = 1.0 \times 10^6$ V/cm and $m_\phi = 2$.

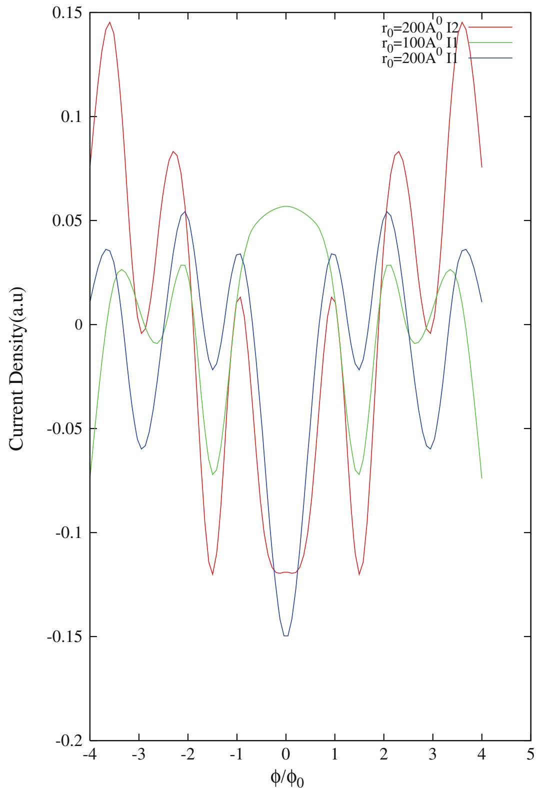

Figure 9. Persistent current density in a quantum ring vs. m_ϕ for intensity $I1$ with $E_0 = 1.0 \times 10^6$ V/cm and $I2$ with $E_0 = 1.5 \times 10^6$ V/cm and ring radius $r_0 = 200$ Å and 100 Å.

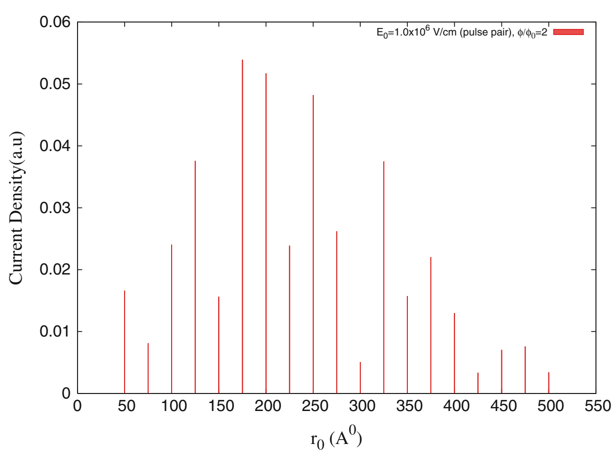

Figure 10. Persistent current density in a quantum ring vs. the ring dimensions for $\phi/\phi_0 = 2$.

and in figure 11 the current density has been plotted as a function of time delay between pulses and the current density is oscillating in nature. Similar results on persistent current density calculation have earlier also been reported [48–50].

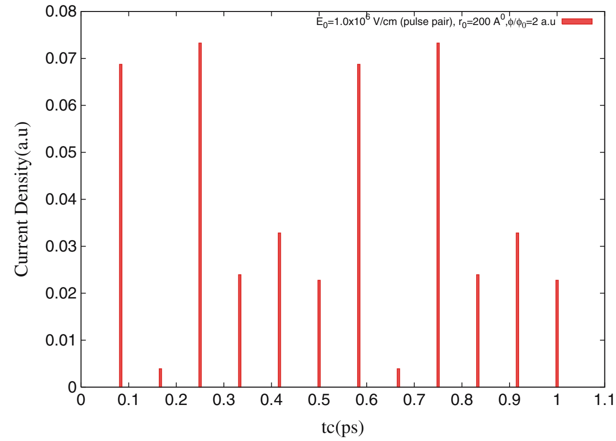

Figure 11. Persistent current density in a quantum ring vs. the pulse delay between two pulses of equal width for a fixed ring radius $r_0 = 200$ Å, $E_0 = 1.0 \times 10^6$ V/cm, $\phi/\phi_0 = 2$.

4. Summary and conclusion

Our work shows that a suitable magnetic field can be used to tune the energy of the electron in the quantum ring. Thus, the optical property of a structure can also be controlled over a given range of wavelength. Further, the transition probabilities can be controlled not only by an appropriate laser field but also by the application of a static magnetic field. These features can be used to externally control the energy spectra and the amplitude of the persistent current.

Acknowledgement

The authors are thankful to the referee for the positive enlightening comments and suggestions which have greatly helped them to improve the manuscript.

References

[1] M Manninen, S Viefers and S M Reimann, *Physica E* **46**, 119 (2012)
[2] E C Niculescu, N Eseanu and A Radu, *Opt. Commun.* **294**, 276 (2013)
[3] G Liu, K Guo and J H Wu, *Superlattices and Microstructures* **57**, 102 (2013)
[4] B Dahiya, V Prasad and K Yamashita, *J. Lumin.* **136**, 240 (2013)
[5] V Prasad and P Silotia, *Phys. Lett. A* **375**, 3910 (2011)
[6] Z-G Zhu and J Berakdar, *J. Phys. Condens. Matter* **21**, 145801 (2009)
[7] S Akgül, M Sahin and K Köksal, *J. Lumin.* **132**, 1705 (2012)
[8] M Sahin and K Köksal, *Semicond. Sci. Technol.* **27**, 125011 (2012)
[9] B Gönül, E Bakir and K Köksal, *Int. J. Theor. Phys.* **47**, 3091 (2008)
[10] A G Aronov and Yu V Sharvin, *Rev. Mod. Phys.* **59**, 755 (2004)

[11] B Gönül, K Köksal and E Bakir, *Physica E* **31**, 148 (2006)
[12] H D Kim, K Kyhm, R A Taylor, G Nogues, K C Je, E H Lee and J D Song, *Appl. Phys. Lett.* **102**, 033112 (2013)
[13] N Li, K Guo and S Shao, *Opt. Commun.* **285**, 2734 (2012)
[14] P-F Loos and P M W Gill, *Phys. Rev. Lett.* **108**, 083002 (2012)
[15] E C Niculescu, *J. Lumin.* **132**, 585 (2012)
[16] S Viefers, P Koskinen, P S Deo and M Manninen, *Physica E* **21**, 1 (2004)
[17] G F Quinteiro and J Berakdar, *Opt. Exp.* **17**, 20465 (2009)
[18] A S Moskalenko, A Matos-Abiague and J Berakdar, *Phys. Rev. B* **74**, 161303 (2006)
[19] A Matos-Abiague and J Berakdar, *Phys. Rev. Lett.* **94**, 166801 (2005)
[20] A Matos-Abiague and J Berakdar, *Europhys. Lett.* **69**, 277 (2005)
[21] A Matos-Abiague and J Berakdar, *Phys. Lett. A* **330**, 113 (2004)
[22] M Moskalets and M Büttiker, *Phys. Rev. B* **66**, 45321 (2002)
[23] T Ihn, A Fuhrer, L Meier, M Sigrist and K Ensslin, *Europhys. News* **36**, 78 (2005)
[24] W Ehrenberg and R E Siday, *Proc. Phys. Soc. London Sect. B* **62**, 8 (1949)
[25] S Washburn and R A Webb, *Adv. Phys.* **35**, 375 (1986)
[26] Y Aharonov and D Bohm, *Phys. Rev.* **115**, 485 (1959)
[27] N Byers and C Yang, *Phys. Rev. Lett.* **7**, 46 (1961)
[28] M Buttiker, Y Imry and R Landauer, *Phys. Lett. A* **96**, 365 (1983)
[29] F Hund, *Ann. Phys. (Leipzig)* **32**, 102 (1938)
[30] V Chandrasekhar, R A Webb, M J Brady, M B Ketchen, W J Gallagher and A Kleinsasser, *Phys. Rev. Lett.* **67**, 3578 (1991)
[31] R Deblock, R Bel, B Reulet, H Bouchiat and D Mailly, *Phys. Rev. Lett.* **89**, 206803 (2002)
[32] J-D Lu, B Xu and W Zheng, *Mod. Phys. Lett. B* **26**, 1150033 (2012)
[33] R Landauer and M Buttiker, *Phys. Rev. Lett.* **54**, 2049 (1984)
[34] Y Gefen, Y Imry and M Y Azbel, *Phys. Rev. Lett.* **52**, 129 (1984)
[35] M A Castellanos-Beltran, D Q Ngo, W E Shanks, A B Jayich and J G E Harris, *Phys. Rev. Lett.* **110**, 156801 (2013)
[36] L P Levy, G Dolan, J Dunsmuir and H Bouchiat, *Phys. Rev. Lett.* **64**, 2074 (1990)
[37] V Chandrasekhar, K Hoki and Y Fujimura, *Chem. Phys.* **267**, 187 (2001)
[38] J S Wenzler and P Mohanty, *Phys. Rev. B* **77**, 121102Δ(R) (2008)
[39] D Mailly, C Chapelier and A Benoit, *Phys. Rev. Lett.* **70**, 2020 (1993)
[40] A Fuhrer *et al*, *Nature (London)* **413**, 822 (2001)
[41] A Lorke, R J Luyken, A O Govorov, J P Kotthaus, J M Garcia and P M Petroff, *Phys. Rev. Lett.* **84**, 2223 (2000)
[42] E Ribeiro, A O Goborov, W Carvalho Jr and G Medeiros-Ribeiro, *Phys. Rev. Lett.* **92**, 126402 (2004)
[43] T Chakraborty and P Pietilainen, *Phys. Rev. B* **50**, 8460 (1994)
[44] N A J M Kleemans, I M A Bominaar-Silkens, V M Fomin, V N Gladilin, D Granados, A G Taboada, J M García, P Offermans, U Zeitler, P C M Christianen, J C Maan, J T Devreese and P M Koenraad, *Phys. Rev. Lett.* **99**, 146808 (2007)
[45] S Moskal and B J Spisak, *Acta Phys. Polon. A* **112**, 101 (2007)
[46] L Xiyimg and L Coaxin, *Phys. Scr.* **82**, 035704 (2010)
[47] S Bhattacharya, A Deyasi, S Sen and N R Das, *Int. J. Adv. Comp. Engng. Arch.* **2(2)**, 153 (2012), ISSN: 2248-9452
[48] P A Orellana, M L Ladrón de Guevara, M Pacheco and A Latgé, *Phys. Rev. B* **68**, 195321 (2003)
[49] S K Maiti, J Chowdhury and S N Karmakar, *J. Phys. Condens. Matter* **18**, 5349 (2006)
[50] H F Cheung, Y Gefen, E K Riedel and W H Shih, *Phys. Rev. B* **37**, 6050 (1988)